Asian Journal of Chemistry; Vol. 27, No. 10 (2015), 3900-3906

ASIAN JOURNAL OF CHEMISTRY

http://dx.doi.org/10.14233/ajchem.2015.19070

Synthesis, Surface Morphology and Properties of Polystyrene Modified Synthetic Clay Nanocomposites

AMANI M. ALANSI[1], WAED Z. ALKAYALI[1], MAHA H. AL-QUNAIBIT[1], TALAL F. QAHTAN[2] and TAWFIK A. SALEH[3,*]

[1]Chemistry Department, King Saud University, Riyadh 12372, Saudi Arabia
[2]Physics Department, King Fahd University of Petroleum & Minerals, Dhahran 31261, Saudi Arabia
[3]Chemistry Department, King Fahd University of Petroleum & Minerals, Dhahran 31261, Saudi Arabia

*Corresponding author: Fax: +966 13 8601734; E-mail: tawfik@kfupm.edu.sa; tawfikas@hotmail.com

Received: 30 January 2015; *Accepted*: 15 March 2015; *Published online*: 22 June 2015; AJC-17370

Polystyrene/modified synthetic clay nanocomposites were prepared using direct intercalation method with the ultra-sonication, as a mean for blending. The advantage of this method is that polymer directly is added to the modified synthetic clay without the need of exfoliating the modified clay before adding polystyrene. The structure, morphology and thermal stability of the prepared materials were investigated by particle size distribution analysis, X-ray diffraction, Fourier transform infrared spectroscopy, scanning electron microscopy, field emission transmission electron microscopy and thermogravimetric analysis. The synthesized nanocomposites showed disordered dispersion of the clay layers in the polystyrene matrix at nanometer level scale, indicating the formation of exfoliated nanostructures with significant improvement in their thermal stability. The nanocomposites show enhanced thermal stability about 17 °C higher than that of pure polystyrene which is attributed to the well dispersion and exfoliation of modified clay at nanometer level scale in the polystyrene matrix.

Keywords: Composites, Chemical synthesis, Scanning tunneling microscopy, TG analysis, Transmission electron microscopy.

INTRODUCTION

Synthetic clay, generally known as layered double hydroxides (LDHs), has become a promising materials using nanofiller for the preparation of polymer nanocomposites since they may offer new opportunities to complement or replace layered silicate materials which are known as cationic clay. There are many applications based on LDHs in several fields, such as in catalysis[1], optical materials[2], separation science[3], DNA reservoirs[4] and flame-retardants[5]. There are three significant properties of LDHs, which make them good nanofillers. The first two properties are their availability in a wide range of chemical compositions and their ease of modification using different types of organic anions. These properties make LDHs appropriate for the production of multifunctional nanohybrids[6-8], improving the mechanical properties of polymer[9], purification of water[10] and enhancement stability of polymer for ultra violet irradiation[11]. The third property is their ability to produce water vapour and metal oxide residues during the endothermic decomposition reactions[12-14] that makes them useful in increasing the thermal stability and flame-retardancy of polymer[15]. The crystal structure of synthetic clay compounds has positively charged layers of metal oxide/hydroxide with intercalated anions and water molecules as shown in Fig. 1[16-20].

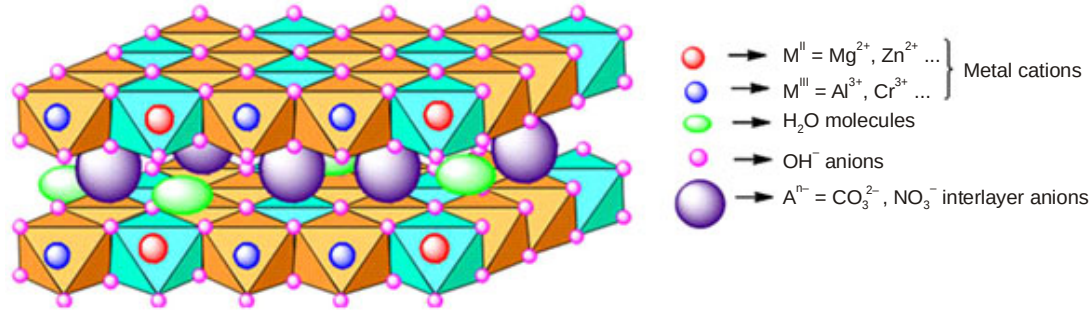

Fig. 1. Layered crystal structure of synthetic clay compounds (LDHs)

Polystyrene (PS) is used in huge quantities in the manufacture of bottles, toys, packaging for food at high temperature and medical supplies such as test tubes holders and Petri dishes. The thermal stability of the polystyrene is a challenge in some applications. The addition of inorganic layered materials such as synthetic clay (LDH) is an effective way to get better thermal stability. Layered double hydroxides can be modified *via* an appropriate long chain of organic anions such as the salts of carboxylates, sulfonates, sulfates and phosphates due to their difficulty exfoliation in the organic polymer matrix. The organic modification increases the interlayer intervals of LDH layers and makes them more hydrophobic[21,22]. The good dispersion of the LDH nanolayers within the polymer matrix is the most important factor that helps to improve many properties, such as mechanical[23-25], gas barrier[26], thermal and flame retardant properties[27,28]. There are two structures of nanocomposites that can be realized as a result of the dispersion of the nanopartials of clay in a polymer matrix[21]. Firstly, intercalated structures are formed due to the insertion of the polymer chains between the clay layers, which causes a slight increase in the interlayer intervals while retaining the regularly spaced stack layers. Secondly, exfoliated structures are obtained when the clay layers can overcome the forces of attraction between them and disperse randomly in the polymer matrix[22].

Recently, the preparation and properties of many polystyrene/organo-modified clay nanocomposites have been reported[26-29]. Direct intercalation method was used to prepare PS/ZnAl LDH nanocomposites using intercalated SDS and xylene as a solvent. The PS/ZnAl LDH nanocomposites showed an improvement in the thermal stability[26]. In addition, a series of PS/OLDH nanocomposites can be prepared by the solvent mixing method[29]. Paul *et al.*[27] reported the preparation of polystyrene/laponite nanocomposites by intercalation of the polystyrene chain into the organo-laponite. Mashael *et al.*[28] synthesized intercalated polystyrene/organo-montmorillonite polystyrene/(O-MMT) nanocomposites by the solution method using different sonication times.

In this present study, firstly, the modified synthetic clay (LDH) was synthesized using organic anion SDS (sodium dodecyl hydroxide), which was intercalated into the LDH gallery by the co-precipitation method. Secondly, polystyrene (PS)/modified synthetic clay (SDS-LDH) nanocomposites were prepared using simple, cost effective and the fastest (15 min) and most direct intercalation method by ultrasonication as a means for blending and studying their thermal stability. To the best of our knowledge, there is no research on the synthesis of polystyrene nanocomposites based on modified synthetic clay by using power ultrasonic waves. The advantage of this method is to directly add the polymer to the SDS-LDH without the need of exfoliating the SDS-LDH before adding polystyrene. In comparison with other studies[23,25-29], this will save more time. Also, the blending process in toluene requires a little quantity of clay and this may be given a good blending of clay and polymer. The main purpose of the present work has been devoted to study the effect of modified synthetic clay (SDS-LDH) and power ultrasonic waves in the structural, morphological as well as thermal stability of the polystyrene matrix. The structure, morphology and thermal stability of the prepared samples were determined by different analytical equipment.

EXPERIMENTAL

To render the hydrophobic clay surface, it is intercalated with organic anions such as alkyl sulfate salt by a co-precipitation method. Sodium dodecyl sulfate (SDS) with a molecular weight of ($NaC_{12}H_{25}SO_4$, Mw = 288.38 g/mol), which was used as a surfactant, was supplied by WINLAB. Polystyrene was used as a matrix and was provided by the Saudi Basic Industries Corporation (SABIC) (Mw = 259,000 g/mol) and the trade name was PS125.

The other reagents such as toluene, $Mg(NO_3)_2{\cdot}6H_2O$ and ($Al(NO_3)_3{\cdot}9H_2O$, NaOH, ethanol) were received from AVONCHEM, LOBA and BDH respectively.

Preparation of sodium dodecyl sulfonate intercalated MgAl-LDH: Sodium dodecyl sulfonate (SDS) intercalated LDHs were prepared by a co-precipitation method at a constant pH. A solution (A) was a mixture of (0.75 M, 60 mL) $Mg(NO_3)_2{\cdot}6H_2O$ and of (0.25, 60 mL) $Al(NO_3)_3{\cdot}9H_2O$. A second solution (B) was (NaOH concentration 1 M).A third solution (C) was (0.6 M, 86.5 g) of SDS. Solutions A and B were added drop-wise to solution C with constant stirring and heating at 75 °C. The pH value was kept at 9 by adding NaOH solution (1 M). Addition was completed in 8 h. The obtained precipitate was aged under the same conditions for 24 h in order to obtain well crystallized and uniform particle size distribution. Then it was filtered by centrifugation being washed four times using deionized water at the same time and dried in an oven at 60 °C for 1 day. The schematic diagram of the experimental steps used to synthesize SDS-LDH is depicted in Fig. 2.

Preparation PS/SDS-LDH nanocomposites: An aqueous solution of polystyrene was prepared by dissolving polystyrene in toluene at 25 °C. PS/SDS-LDH aqueous solution with (0.5, 1, 2 and 4 % wt SDS-LDH loadings) was prepared through direct intercalation using ultrasonication. Firstly, a desired amount of SDS-LDH prepared already was added into 10 mL toluene and 10 mL of polystyrene/toluene solution was added to the SDS-LDH solution. Secondly, the mixture of polymer and clay was sonicated in an ultrasonic bath for 15 min at room temperature. Finally, the mixture was poured into 100 mL of cool ethanol to obtain the prepared nanocomposites. Cool ethanol leads to rapid precipitation in order to avoid aggregation of the LDH layers. After sample filtering, the synthesized precipitate was dried for two days at 100 °C.

The schematic diagram of the experimental steps used to synthesize the aqueous suspensions of PS/SDS-LDH is shown in Fig. 3.

Experimental procedure: Particle size dispersion measurements of SDS-LDH suspensions were performed using Malvern Zetasizer, ZS and ZEN3500 (UK). Powder X-ray diffraction (PXRD) patterns were recorded in a Rigaku Miniflex II diffractometer with Cu radiation (30 kV, 15 mA) equipped with Ni-filter. The scanning speed was 2 °/min. In order to confirm the type of bonding in the prepared samples, the FTIR spectrum was measured and recorded on the FTIR system spectrum BX from Perkin-Elmer with dry KBr as standard reference in the range of 4000-400 cm^{-1}.

For surface morphology studies the field emission scanning electron microscopy (FESEM, model JEOL JSM

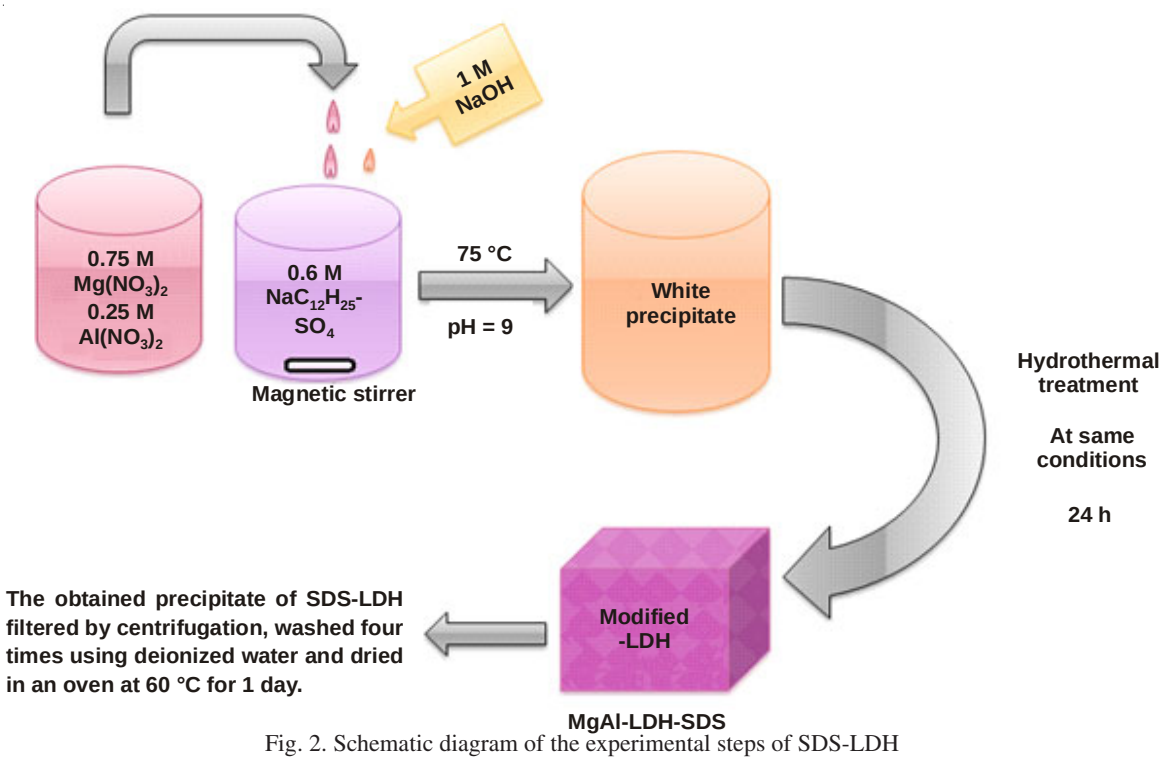

Fig. 2. Schematic diagram of the experimental steps of SDS-LDH

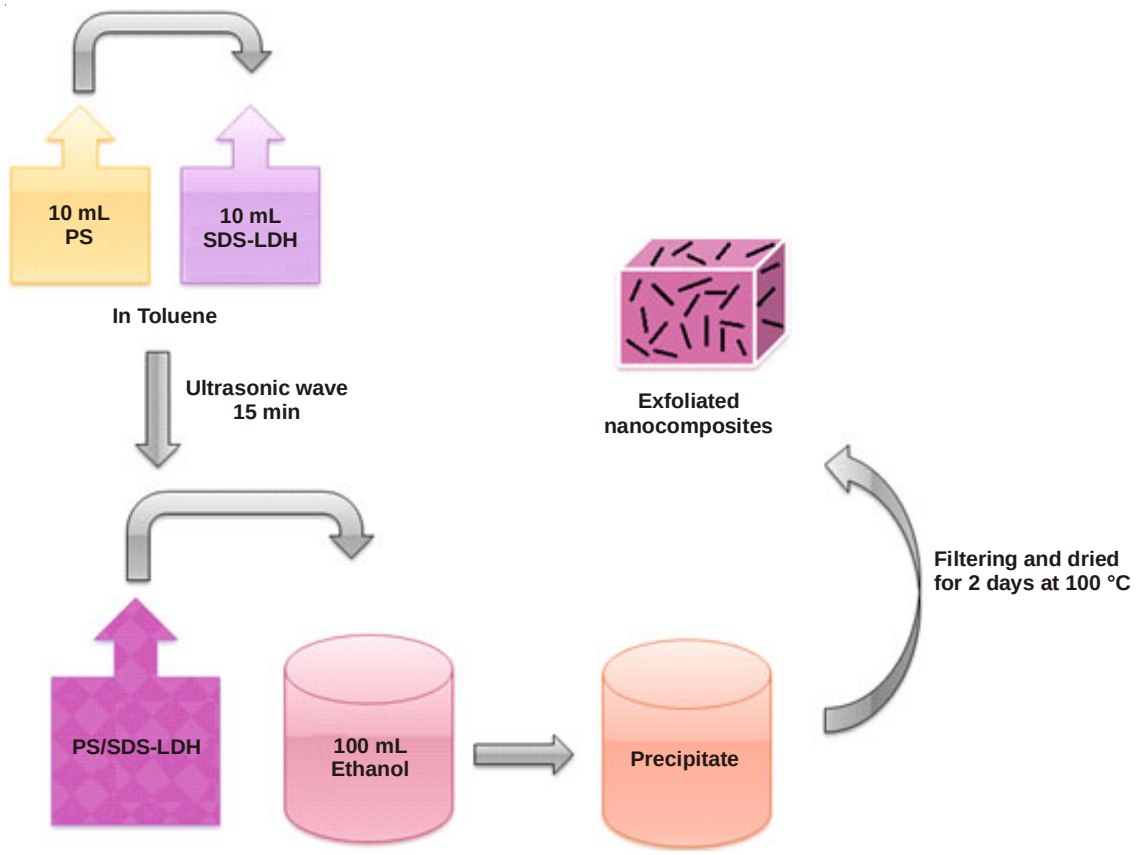

Fig. 3. Schematic diagram of the experimental steps of PS/SDS-LDH

7600F) was used by operating at 15 kV with different magnification powers. The sample was sputter-coated with platinum before examining under the microscope. To observe the state of dispersion of the LDH particles in the polystyrene matrix, field emission transmission electron microscope (TEM, JEOL JEM-2100F) was used at different magnification. TEM was carried out at room temperature with an acceleration voltage of 200 kV and bright field illumination. The thermogravimetric analysis of the prepared samples was carried out on TGA Q500 V20.13 Build 39 instrument using approximately 10 mg of

sample. The analysis was recorded from 25 to 1000 °C at a heating rate of 10 °C min^{-1} under nitrogen flow.

RESULTS AND DISCUSSION

Size Distribution of SDS-LDH: Particle size distribution analysis (PSD) was applied to give good information about the size and range of a set of particles in the clay. Particle size was determined using dynamic light scattering measurements. The diagram of the size distribution of SDS-LDH suspension is shown in Fig. 4. The Zetasizer software uses algorithms to read out the decay rates for a number of size classes to get a size distribution. The X-axis illustrates a distribution of size classes, whereas the Y-axis illustrates the relative intensity of the scattered light. The particle size-distribution curve shows one peak distribution in the range 30-45 nm size with a narrow size distribution, which may be evidence that the size of most SDS-LDHs particles ranges from 30 to 45 nm. The poly-dispersity index for the SDS-LDH is considerably narrow at about 0.4. Previous results demonstrated that the particle size of SDS-LDH has a lower monodispersal, indicating that they have not the same size and shape.

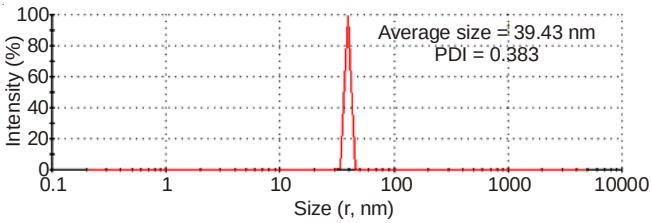

Fig. 4. Particle size distributions of the SDS-LDH suspension

X-Ray diffraction: When the interlayer spacing (d) of the LDH increases to a few nanometers, it indicates the formation of an intercalated structure. But in case of the full loss of registry between the clay layers such that there is no peak appearance in the XRD patterns that usually indicates an exfoliated structure was formed. The structural characteristics of LDH, SDS-LDH, PS/SDS-LDH nanocomposites (0.5, 1, 2 and 4 % wt loading of SDS-LDH) and unfilled polystyrene were determined by using X-ray diffraction (XRD), which was shown in Fig. 5. The position of the basal peak (003) indicates the interlayer spacing between two metal hydroxide sheets (d003). The basal reflection (003) of SDS-LDH has the value of 2θ about 3.03° (according to the Bragg law) which corresponds to a basal spacing or interlayer distance of about 2.90 nm. According to the previous result, the large distance between the SDS-LDH layers facilitated the exfoliation of the stacked layers in the polymer matrix to produce PS/SDS-LDH nanocomposites[30]. In XRD pattern of polystyrene there are two peaks, the first one was observed at about 10°. The second broad peak appeared at about 25 = 20°. In the case of the PS/SDS-LDH nanocomposites, all XRD patterns showed as an amorphous structure and no clear crystallization peak can be observed. However, another two peaks were observed in the XRD patterns of nanocomposites. Generally, the full disappearance of any crystalline XRD peaks may be due to the breakdown of the stacked platelets of LDH structure, leading to the formation of a random and exfoliated nanostructure within the polystyrene matrix[23,30,31]. In other words, the SDS-LDH

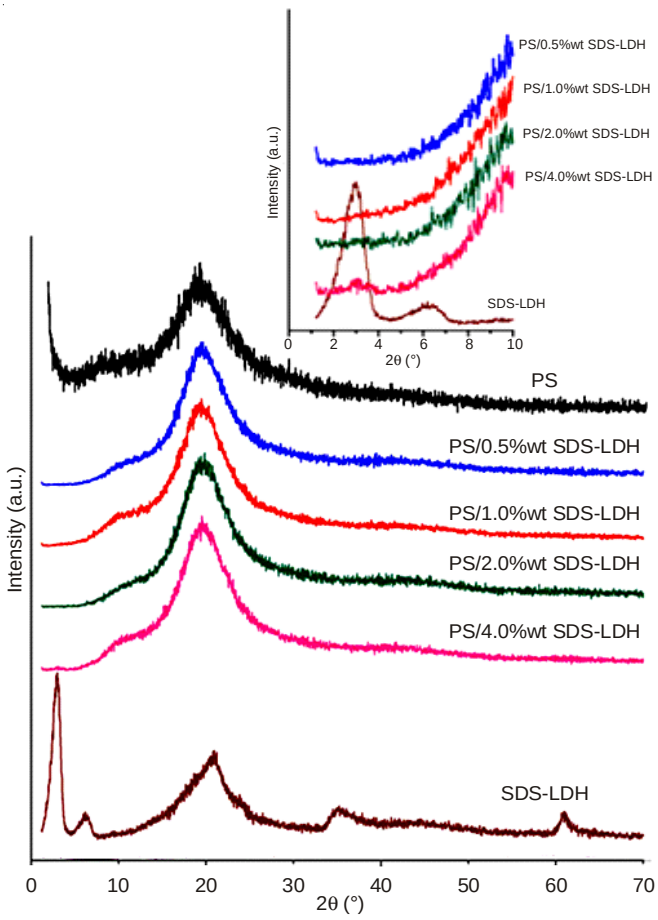

Fig. 5. XRD patterns of LDH, SDS-LDH, PS/SDS-LDH nanocomposites and polystyrene

layers were disorderedly dispersed throughout the polystyrene matrix.

Infrared spectra: FTIR analysis is applied to give some information about the structural bonding and chemical properties of PS/SDS-LDH nanocomposites. The FTIR spectra of SDS-LDH, PS/SDS-LDH nanocomposites and polystyrene are depicted in the overlap spectra (Fig. 6). In the SDS-LDH spectrum, a broad band appears at approximately (3600-3300 cm^{-1}) due to the stretching frequency of hydrogen-bonded OH groups in the hydroxyl layers of LDH and absorbed water[32]. On the other hand, the bending OH vibration mode of water molecules is centered at 1635 cm^{-1}. The several absorption bands that appeared in (800-400 cm^{-1}) region may be assigned to (Mg–O, Al–O) and (O–Mg–O O–Al–O) modes which are known as the lattice vibration bands. The absorption bands at around 2923 and 2854 cm^{-1} corresponded to the stretching vibration of CH_2 and CH_3 respectively, which are present in the organic chain of the SDS. The band located at 1468 cm^{-1} can be attributed to C–H bending vibration[23,33]. Symmetric and asymmetric stretching vibrations bands of the sulfate (SO_4^{2-}) group were observed[34] around 1210 and 1062 cm^{-1}. These results confirm that the SDS has been intercalated in LDH layers. Polystyrene included several absorption bands that appeared at different positions in the infrared spectrum. They are located at 3060, 3028, 2916, 2852, 1945-1670, 1600-1448, 1371-1856, 1070-1026, 759-699 and 543 cm^{-1} and the explanations of these absorption bands were reported[28]. Clearly,

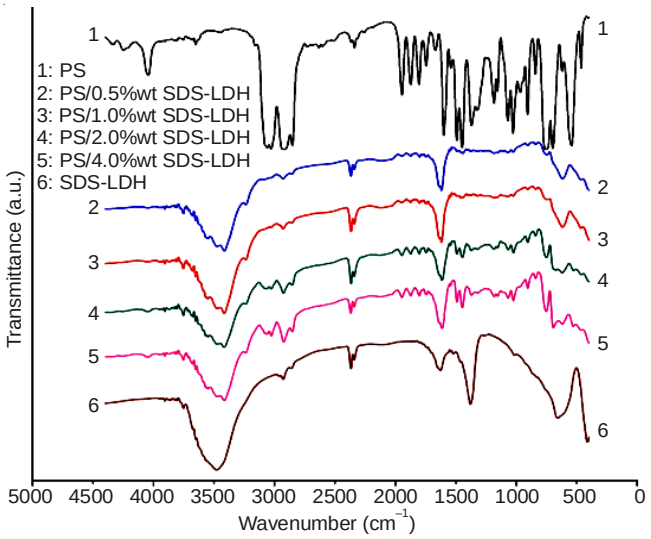

Fig. 6. FTIR spectra of SDS-LDH, PS/SDS-LDH nanocomposites and polystyrene

the FTIR spectra of the PS/SDS-LDH nanocomposites with all loading SDS-LDH exhibited the characteristic absorption bands that were attributable to polystyrene and SDS-LDH. There were few absorption bands of polystyrene appearing in the spectra of the nanocomposite samples with low intensity. On the other hand, many SDS-LDH absorption bands appeared in the nanocomposites spectra with a slight shifting, such as the bands that appeared in the areas of 3415, 1617 and 619 cm^{-1} which were attributed to OH stretching, H_2O bending and SDS-LDH bending respectively. These results indicated the existence of SDS-LDH in the polystyrene matrix.

Morphological characterization of SDS-LDH: For the morphology investigation of the synthesized materials, scanning electron microscopy (SEM) and field emission transmission electron microscope (TEM) techniques were applied to investigate the morphology of the particles of the prepared SDS-LDH. The images of both SEM and TEM for SDS-LDH sample are shown in Fig. 7a and 7b, respectively. The particles of prepared SDS-LDH appeared to be mostly large, plate-like and irregular in shape. The TEM image of the prepared SDS-LDH showed many aggregated platelets with undefined shapes, small in size and stacked orderly.

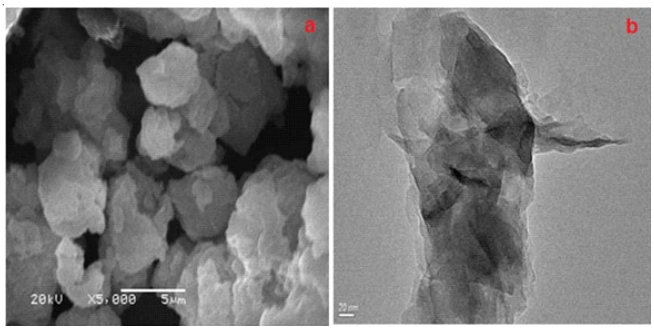

Fig. 7. (a) SEM and (b) TEM images of SDS-LDH

Morphological characterization of PS/SDS-LDH nanocomposites: Besides useful XRD analysis, TEM is a powerful instrument that can be directly used to describe how the clay layers are distributed in the polymer matrix. Therefore, TEM can be used to reveal the exact intercalation or exfoliation degree of the filler in the polymer matrix. Fig. 8a and 8b show TEM images of PS/SDS-LDH nanocomposites with 0.5 and 4 wt % SDS-LDH loadings, respectively. The SDS-LDH layers appeared as dark lines distributed in the polymer matrix which appeared as a gray area. TEM images of PS/SDS-LDH nanocomposites showed completely different morphology from the TEM image of SDS-LDH in Fig. 7 and the original stacked lamellar structure of SDS-LDH layers can be significantly degrade to form the randomly dispersed morphology at the nanometer scale in the polystyrene matrix. The result of the TEM analysis suggested that the clay layers have been exfoliated in the polystyrene matrix during the sonication process and these results agree with the results that were reported from the XRD characterization. This result shows the effectiveness of the ultrasonic waves in the formation of the exfoliated structure of nanocomposites.

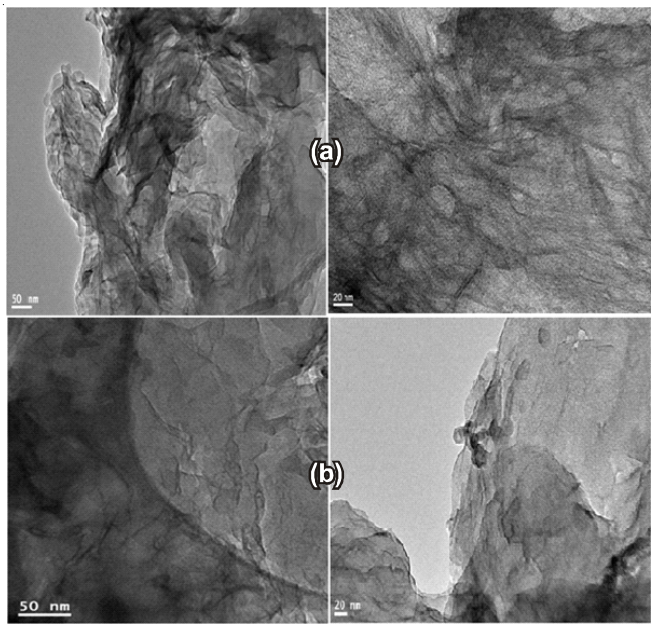

Fig. 8. TEM images of (a) PS/0.5 % wt. SDS-LDH and (b) PS/4 % wt. SDS-LDH nanocomposites

TGA analysis: The TGA curve (Fig. 9) of the degradation of SDS-LDH is divided into four stages. The first one was assigned in the below (120 °C/mass loss 8 %) can be ascribed to the evaporation of adsorbed water. The second stage ranging (120-250 °C/mass loss 37.4 %) is attributed to the degradation of organic chain of SDS in the LDH. The third stage ranging (250-520 °C/mass loss 13.6 %) is because of the dehydroxylation of LDH layers. The degradation temperature of dehydroxylation increases because it is hindered by the second step. The fourth stage began at (570 and ended at 800 °C/mass loss 8.5 %) is proposed that this could be the result of the decomposition of remains magnesium sulfate salt resulting from the decomposition of SDS chain and formation the mixtures of metal oxides. The total mass loss of SDS-LDH for the region (25-800 °C) is 67.5 %. The residual chars SDS-LDH was calculated to be 32.5 %.

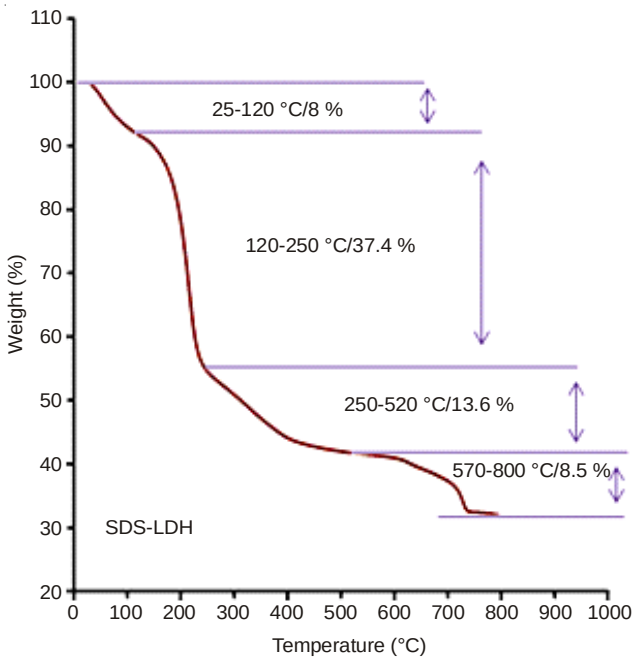

Fig. 9. TGA of SDS-LDH

The thermal behaviour of unfilled polystyrene was divided into one-step, (about 250-450 °C) which was attributed to the thermal decomposition of the polystyrene backbone. All the PS/SDS-LDH nanocomposite samples exhibited a similar tendency to thermal decomposition for unfilled polystyrene because they thermally decomposed in one stage. This decomposition was due to the degradation of the backbone of the polystyrene chain and SDS-LDH alkyl chain. Usually, the comparison of thermal stability for polymeric materials from TGA plots is carried out in terms of two temperatures: one is the onset of the decomposition temperature ($T_{0.10}$) at which 10 % weight loss takes place and the other is the decomposition temperature ($T_{0.50}$) at which 50 % weight loss takes place. The degradation temperature at 10 % and 50 % ($T_{0.1}$ and $T_{0.5}$) were selected as a point of comparison between the $T_{0.1}$ and $T_{0.5}$ of unfilled polystyrene and the $T_{0.1}$ and $T_{0.5}$ of PS/SDS-LDH nanocomposites containing 0.5, 1, 2 and 4 % wt SDS-LDH. The TGA curves of PS/SDS-LDH nanocomposites and polystyrene were illustrated in Fig. 10. The $T_{0.1}$ was determined as 363, 370, 372, 378 and 380 °C, respectively. In addition, the degradation temperatures $T_{0.5}$ for the polystyrene and all nanocomposites were398, 406, 410, 412 and 414 °C, respectively. These results implied that at 10 wt % and 50 wt % losses, the PS/SDS-LDH nanocomposites show a higher thermal stability of 7-17 °C and 8-16 °C in comparison with pure polystyrene. The $T_{0.1}$ and $T_{0.5}$ of PS/SDS-LDH nanocomposites increased regularly with the increase of the SDS-LDH content in the nanocomposites. The nanocomposite samples, even those that contain a small amount of SDS-LDH, exhibit an improvement in the thermal stability relative to unfilled polymer. This improvement is attributed to the presence of SDS-LDH residues at the polystyrene surface that obstructs the internal diffusion of heat and gaseous small molecules formed during thermal oxidation that acts as an isolator and protects the bulk polymer[10,11]. In addition, ultrasonication facilitated the dispersion and exfoliation of SDS-LDH in the polystyrene matrix and thus enhanced the thermal stability. The residues were increased according to the increase for SDS-LDH in the nanocomposites and this is enough to enhance the thermal stability of these nanocomposites. According to the results of both XRD and FETEM, the suitable mechanism for the formation of PS/SDS-LDH nanocomposites *via* ultrasonic method is illustrated in Fig. 11.

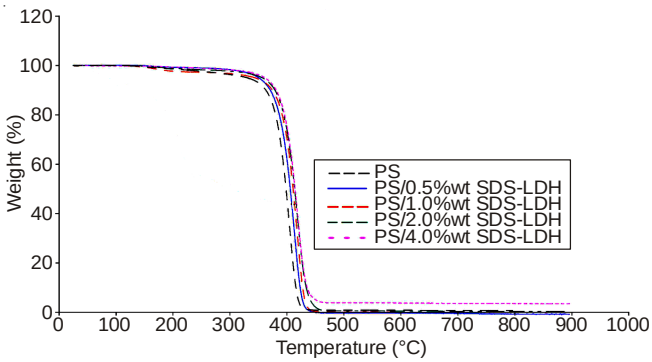

Fig. 10. TGA of PS/SDS-LDH nanocomposites and polystyrene

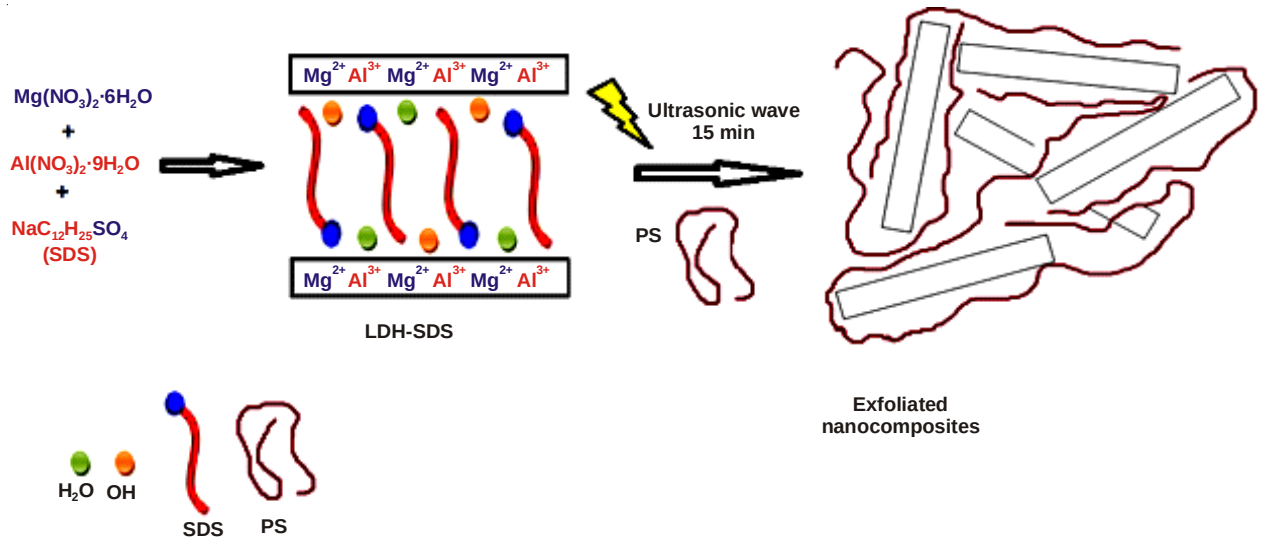

Fig. 11. Scheme of the SDS-MgAl LDH nanocomposites prepared through the direct intercalation method using ultrasonic waves

Conclusion

PS/SDS-LDH nanocompositeswere successfully prepared by dispersing the modified synthetic clay, commonly known as layered double hydroxides, in polystyrene through a direct intercalation method by using ultrasonic waves. The modified LDH was synthesized using SDS anions, which intercalated into the LDH gallery by the co-precipitation method. The results of FTIR, XRD, FESEM, FETEM and TGA analyses were investigated. Both of XRD and FETEM measurements illustrated a disorderly dispersion of layered clay in the polystyrene matrix at a nano scale, indicating the formation of exfoliated nanocomposites. The TGA analysis showed a clearer improvement in the thermal stability of polystyrene nanocomposites than the unfilled polystyrene. The ultrasonication process facilitated the dispersion and exfoliation of SDS-LDH in the polystyrene and thus enhanced thermal stability of the nanocomposites.

ACKNOWLEDGEMENTS

This research project was supported by a grant from the "Research Center of Female Scientific and Medical Colleges", Deanship of Scientific Research, King Saud University, Riyadh, Saudi Arabia.

REFERENCES

1. S. Bhattacharjee and A.J. Anderson, *Chem. Commun.*, **5**, 554 (2004).
2. M. Ogawa and K. Kuroda, *Chem. Rev.*, **95**, 399 (1995).
3. A.M. Fogg, V.M. Green, H.G. Harvey and D. O'Hare, *Adv. Mater.*, **11**, 1466 (1999).
4. J.H. Choy, S.Y. Kwak, Y.J. Jeong and J.S. Park, *Angew. Chem. Int. Ed.*, **39**, 4041 (2000).
5. B. Du, Z. Guo and Z. Fang, *Polym. Degrad. Stab.*, **94**, 1979 (2009).
6. B. Li, J. He, D. Gevans and X. Duan, *Appl. Clay Sci.*, **27**, 199 (2004).
7. L.P. Cardoso, R. Celis, J. Cornejo and J.B. Valim, *J. Agric. Food Chem.*, **54**, 5968 (2006).
8. J.H. Choy, S.Y. Kwak, J.S. Park and Y.J. Jeong, *J. Mater. Chem.*, **11**, 1671 (2001).
9. H.B. Hsueh and C.Y. Chen, *Polymer*, **44**, 5275 (2003).
10. S. Jin, P.H. Fallgren, J.M. Morris and Q. Chen, *Sci. Technol. Adv. Mater.*, **8**, 67 (2007).
11. S. Guo, D.G. Evans and D. Li, *J. Phys. Chem. Solids*, **67**, 1002 (2006).
12. S. Carlino, *Solid State Ion.*, **98**, 73 (1997).
13. M. Meyn, K. Beneke and G. Lagaly, *Inorg. Chem.*, **29**, 5201 (1990).
14. V. Prevot, C. Forano and J.P. Besse, *Appl. Clay Sci.*, **18**, 3 (2001).
15. L. Qiu, W. Chen and B. Qu, *Polymer*, **47**, 922 (2006).
16. V. Rives and M.A. Ulibarri, *Coord. Chem. Rev.*, **181**, 61 (1999).
17. S.K. Yun and T.J. Pinnavaia, *Chem. Mater.*, **7**, 348 (1995).
18. Z. Liu, R. Ma, M. Osada, N. Iyi, Y. Ebina, K. Takada and T. Sasaki, *J. Am. Chem. Soc.*, **128**, 4872 (2006).
19. V. Rives, Layered Double Hydroxides: Present and Future, Nova Publishers, New York, p. 439 (2001).
20. F. Cavani, F. Trifirò and A. Vaccari, *Catal. Today*, **11**, 173 (1991).
21. P. Ding and B. Qu, *J. Polym. Sci. B, Polym. Phys.*, **44**, 3165 (2006).
22. T. Kuila, H. Acharya, S.K. Srivastava and A.K. Bhowmick, *J. Appl. Polym. Sci.*, **108**, 1329 (2008).
23. H. Peng, Y. Han, T. Liu, W.C. Tjiu and C. He, *Thermochim. Acta*, **502**, 1 (2010).
24. Q. Wang, X. Zhang, C.J. Wang, J. Zhu, Z. Guo and D. O'Hare, *J. Mater. Chem.*, **22**, 19113 (2012).
25. J. Liu, G. Chen and J. Yang, *Polymer*, **49**, 3923 (2008).
26. L. Qiu, W. Chen and B. Qu, *Polym. Degrad. Stab.*, **87**, 433 (2005).
27. P.K. Paul, S.A. Hussain, D. Bhattacharjee and M. Pal, *Bull. Mater. Sci.*, **36**, 361 (2013).
28. A. Mashael, A. Al-Arrash and W. Mekhamer, *J. Nanomater.*, Article ID 650725 (2013).
29. B. Sahu and G. Pugazhenthi, *J. Appl. Polym. Sci.*, **120**, 2485 (2011).
30. S.P. Lonkar, S. Morlat-Therias, N. Caperaa, F. Leroux, J.L. Gardette and R.P. Singh, *Polymer*, **50**, 1505 (2009).
31. S. Guo, C. Zhang, H. Peng, W. Wang and T. Liu, *Compos. Sci. Technol.*, **71**, 791 (2011).
32. L. Qiu, W. Chen and B. Qu, *Polymer*, **47**, 922 (2006).
33. F.R. Costa, A. Leuteritz, U. Wagenknecht, D. Jehnichen, L. Häußler and G. Heinrich, *Appl. Clay Sci.*, **38**, 153 (2008).
34. S.P. Lonkar, S. Therias, N. Caperaa, F. Leroux and J.-L. Gardette, *Eur. Polym. J.*, **46**, 1456 (2010).